

## Mechanistic Insights into the Whitening Effect of a Combination of W335 and Tranexamic Acid: Involvement of the Ubiquitin-Proteasome System and Autophagy in Melanogenesis

Zha, Fanglan<sup>1</sup>; Wei, yun<sup>1</sup>; Lin, Simin<sup>1</sup>; Mu, Jian<sup>1</sup>; Liu, Xingyu<sup>1</sup>; Xuan, Lingling<sup>1</sup>; **Wang, Jing**<sup>1\*</sup>;

<sup>1</sup> Proya Cosmetics Co., Ltd, Hangzhou, 310012, China

\* Wang, Jing; Address: Proya Cosmetics Co., Ltd, Hangzhou, 310012, China; Telephone: +86-18768141851; Email: wangjing48@proya.com

### Abstract

In Asia, fair skin is considered a symbol of youth and beauty, leading to a high demand for skin whitening cosmetics in the market. Our previous work chemically synthesized a new cosmetic ingredient, 3,3,5-trimethylcyclohexyl succinate dimethylamide (W335). This study developed a novel whitening agent combination [W335 + tranexamic acid (TXA)] and investigated its efficacy and mechanism on melanogenesis. The whitening effect of the agent combination was evaluated by measuring melanin content in human keratinocytes (HaCaT) and mouse melanoma cells (B16). Transcriptome sequencing was performed to elucidate the pathways by which W335 regulates melanogenesis. Melanosomes were isolated from human melanoma cells (MNT-1) and co-cultured with keratinocytes to validate the specific mechanisms. W335 and TXA combination (1:10) significantly reduced the melanin content in B16 cells compared to individual treatments. Transcriptomic data revealed the involvement of W335 in the ubiquitin-proteasome system (UPS) and autophagy pathway. *In vitro* experiments confirmed that W335 and TXA combination inhibited melanin production by promoting ubiquitination degradation of tyrosinase and autophagic degradation of melanosomes. This study showed that W335 and TXA combination exerted the whitening effect by regulating UPS and autophagy pathway. These findings highlight the potential application of W335 and TXA combination in cosmetics to elevate whitening efficacy.

**Keywords:** Melanin; Ubiquitin-Proteasome System; Autophagy; W335; Tranexamic acid

## Introduction.

Melanocytes originate from multipotent neural crest cells and are present in various tissues throughout the body [1]. Melanin, an endogenously synthesized pigment molecule within melanocytes, constitutes the primary pigment in mammalian skin and hair [2]. Melanogenesis is a complex process influenced by a myriad of extrinsic and intrinsic factors such as hormonal changes, inflammation, age, and exposure to ultraviolet (UV) radiation [3]. Although cutaneous pigmentation serves as a robust defense against UV irradiation [4], excessive melanin production can lead to hyperpigmentation issues, such as melasma, freckles, lentigines, and ephelides [5, 6]. Currently, melanogenesis inhibitors targeting tyrosinase (TYR), including hydroquinone, kojic acid, and their derivatives (e.g., kojic ester derivatives), are widely used in both pharmaceutical and cosmetic products. However, although these agents show good efficacy, prolonged use of them may cause side effects, including irritant dermatitis and exogenous ochronosis [7]. To overcome these limitations, there is an urgent need to develop novel, safer methods for effectively inhibiting melanin production.

The ubiquitin-proteasome system (UPS) and autophagy are two major mechanisms in organisms responsible for protein degradation, regulating critical protein homeostasis and maintaining a healthy intracellular environment [8]. The UPS is a selective proteolytic system where substrates are recognized by the proteasome following tagging with ubiquitin for degradation. The ubiquitination process is primarily mediated by three classes of ubiquitin enzymes: ubiquitin-activating enzyme (E1), ubiquitin-conjugating enzyme (E2), and ubiquitin-protein ligases (E3) [9]. Ubiquitination and deubiquitination maintain ubiquitin homeostasis, which is a highly dynamic equilibrium process under the actions of E3 ubiquitin ligases and deubiquitinating enzymes. It has been reported that ubiquitination and deubiquitination can control melanin production by altering the degradation or stabilization of melanogenic proteins

[10]. Therefore, the exploration of the potential relationship between melanogenesis and UPS is gaining increasing attention.

Autophagy is an integrated degradation system that employs lysosomal hydrolases to degrade proteins and various other cellular components [11]. In mammalian cells, there are three types of autophagy: microautophagy, macroautophagy, and chaperone-mediated autophagy. Although each type differs morphologically, they all share the common feature of delivering cargo to lysosomes for degradation and recycling [12]. Notably, a study revealed that keratinocytes derived from Caucasian skin exhibit higher levels of autophagic activity compared to those from African American skin [13]. Growing evidence suggests the involvement of autophagy-related proteins in the melanogenesis signaling pathways. Amrita et al. demonstrated that classical autophagy proteins such as LC3B and ATG4 facilitate the transport of melanosomes along cytoskeletal tracks [14]. Moreover, certain cosmetic ingredients with whitening efficacy have been shown to reduce skin pigmentation through autophagy induction. For example, the natural phenolic antioxidant ellagic acid has been reported to suppress melanin synthesis in B16 melanoma cells by inducing autophagy [15]. These findings suggest that autophagy may play a crucial role in regulating skin pigmentation.

In our previous work, we prepared the cosmetic ingredient 3,3,5-trimethylcyclohexanol succinate dimethylamide (W335) through chemical synthesis. Here, we further investigate its efficacy and mechanisms on melanogenesis by *in vitro* experiments and transcriptome sequencing. Concurrently, we formulated a composite containing W335 and tranexamic acid (TXA), analyzing their synergistic whitening effects and potential mechanisms. This study deepens insight into skin pigmentation processes and provides new avenues for cosmetic and pharmaceutical applications.

## **Materials and Methods.**

### **Chemicals**

W335 was synthesized by the R&D department of our company (patent No. CN202311103185.4). TXA was purchased from Shanghai YuanYe Biotechnology Co., Ltd. (China). The proteasome inhibitor MG132 was purchased from Absin (China), ubiquitination activator CC122 was obtained from MCE (China), 3-methyladenine (3-MA) was obtained from Sigma (USA), rapamycin was purchased from Solarbio (China), and non-essential amino acids were supplied by CellCook (China).

#### Cell culture

Human immortalized keratinocyte cells (HaCaT), murine melanoma cells (B16), and human melanoma cells (MNT-1) were purchased from the Shanghai Institutes for Biological Sciences, the Chinese Academy of Sciences (China). HaCaT and B16 cells were cultured in high-glucose Dulbecco's modified Eagle medium (DMEM) supplemented with 10% fetal bovine serum (FBS). MNT-1 cells were cultured in high-glucose DMEM containing 20% FBS and 1% non-essential amino acids. Both media were supplemented with 100 U/mL of penicillin and 100 µg/mL of streptomycin. All cells were maintained at 37°C in a humidified atmosphere with 5% CO<sub>2</sub>.

#### Cell viability assay

Cell viability assay was conducted according to the manufacturer's instructions using the Cell Counting Kit-8 (CCK-8, Dojindo Laboratories, Japan). In brief, HaCaT and B16 cells were seeded at a density of 5,000 cells per well into 96-well plates and allowed to adhere overnight without drug treatment. Subsequently, cells were treated with different concentrations of W335 or TXA for 24 h. Following this treatment, the CCK-8 solution was added to each well, and the cells were incubated for 1 h. Absorbance values were then measured at a wavelength of 450 nm using a microplate reader.

#### Measurement of melanin content

B16 cells were seeded into 24-well plates and incubated overnight in a CO<sub>2</sub> incubator (37°C, 5% CO<sub>2</sub>). Upon reaching 40%~50% confluences, cells were divided into four groups: control, rapamycin, 3-MA, and sample groups. In each well, the control group received 500 µL of

culture medium, the rapamycin group received 500 µL of culture medium containing 1 nM rapamycin, the 3-MA group received 500 µL of culture medium containing 1 µM 3-MA, and the sample group, 500 µL of culture medium containing the different concentrations of W335 and/or TXA. Then, the cells were incubated for 48 h, followed by digestion with trypsin. The cells were washed twice with pre-cooled phosphate buffered saline (PBS) and lysed by 100 µL of 1 M NaOH at 80°C for 5 to 10 min until all the melanin was completely dissolved. Cell lysates (70 µL) were transferred to a 96-well plate, and the absorbance (OD) was measured at 405 nm. Melanin content was calculated as: melanin content (%) = OD<sub>sample</sub>/OD<sub>control</sub> × 100%.

#### RNA sequencing

Total RNA was extracted from melanocytes or keratinocytes with or without W335 treatment. Subsequently, rigorous quality control measures were applied to the RNA samples, with the integrity of RNA being precisely assessed using the Agilent 2100 Bioanalyzer. Messenger RNAs (mRNAs) with polyA tails were purified using oligo(dT) magnetic beads and then randomly fragmented using Magnesium RNA Fragmentation Module (NEB, USA). Libraries were prepared using the NEBNext® Ultra™ RNA Library Prep Kit for Illumina®. Post-library construction, an initial quantification was conducted using the Qubit2.0 Fluorometer, followed by dilution of the libraries to a concentration of 1.5 ng/µL. The insert size of the libraries was then examined using the Agilent 2100 Bioanalyzer, ensuring conformity with expectations. The precise quantification of library concentration was accomplished through qRT-PCR (effective concentration  $\geq$  2 nM). Qualified libraries were pooled according to their effective concentrations and the targeted output data volume, proceeding to Illumina sequencing. The mapping information of reads on the reference genome was obtained using the HISAT2 software. Based on the alignment positions of genes on the reference genome, reads counts were tallied for each gene (including newly predicted genes), spanning from the start to the stop codon. Reads with mapping quality scores < 10, those aligned to non-proper pairs, and reads mapping to multiple genomic regions were excluded from the count using the

featureCounts tool within the subread software package. Individual samples underwent quantification of gene expression levels, followed by consolidation into an expression matrix encompassing all samples. Differentially expressed genes (DEGs) were screened based on the criteria  $|\log_2(\text{FoldChange})| \geq 1$  and  $\text{padj} \leq 0.05$  and visualized by volcano plots. Additionally, the clusterProfiler software was employed for Gene Ontology (GO) functional enrichment analysis of DEGs.

#### Co-immunoprecipitation (Co-IP)

B16 cells were collected and lysed by IP lysis buffer (containing 6  $\mu\text{L}$  of HaltTM PIC). Protein concentrations in cell lysates were determined using the BCA method and adjusted to a final concentration of 1  $\mu\text{g}/\mu\text{L}$ . For input, 30  $\mu\text{L}$  of cell lysate was mixed with 6  $\mu\text{L}$  of 5 $\times$  loading buffer and boiled for 5 min. The remaining cell lysates were incubated with IgG or anti-TYR antibodies. Then, 50  $\mu\text{L}$  of protein A/G magnetic beads were added and incubated at room temperature for 1 h. The magnetic beads were washed four times with 500  $\mu\text{L}$  of IP lysis buffer. Finally, bead-binding proteins were diluted using 40  $\mu\text{L}$  of 3 $\times$  SDS-PAGE loading buffer (containing DTT) and subjected to Western blot analysis.

#### Isolation of melanosomes

MNT-1 cells were passaged when reaching 70%-80% confluence and then cultured overnight at 37°C with 5% CO<sub>2</sub>. Cells with a confluence around 90% are harvested and digested using trypsin. Then, cells were collected by centrifugation at 4°C and 1,000  $\times g$  for 10 min and washed twice with cold PBS. Cells ( $5 \times 10^6$ ) were homogenized with 500  $\mu\text{L}$  of cold cell lysis buffer, followed by centrifugation at 4°C and 14,000  $\times g$  for 10 min to collect the supernatant.

#### Co-culture of keratinocytes with melanosomes

Keratinocytes were seeded into 6-well plates and incubated overnight at 37°C with 5% CO<sub>2</sub>. Upon full adherence, the cells were washed twice with PBS, followed by incubation with 4 mL of high-glucose DMEM complete medium containing 5  $\mu\text{g}/\text{mL}$  melanosomes at 37°C with 5% CO<sub>2</sub> for 24 h, until a notable change in coloration was observed.

### Immunofluorescence

B16 and HaCaT cells were seeded onto 24-well plates and incubated at 37°C with 5% CO<sub>2</sub> for 24 h. Next, B16 cells were divided into five groups: (1) the control group (no treatment); (2) the linoleic acid (positive control) group (treatment with linoleic acid); (3) the W335 group (treatment with 0.00075% W335); (4) the TXA group (treatment with 0.0075% TXA); (5) the W335 + TXA group (treatment with 0.00075% W335 and 0.0075% TXA). B16 cells in each group were further incubated for 72 h. HaCaT cells were divided into four groups: (1) the control group received 1 mL of fresh medium containing melanosomes; (2) the rapamycin group received 1 mL of fresh medium containing both melanosomes and rapamycin; (3) the hydroxychloroquine group received 1 mL of fresh medium containing melanosomes and hydroxychloroquine; and (4) the sample group received 1 mL of fresh medium containing melanosomes and 0.006% (w/w) W335. HaCaT cells in each group were further incubated for 48 h. Following incubation, cells were fixed with 4% paraformaldehyde. B16 cells were incubated with primary antibodies against UBQLN1 and TYR, followed by incubation with secondary antibody. HaCaT cells were incubated with primary and secondary antibodies against melanosomes, followed by incubations with primary and secondary antibodies against LC3B. Nuclei of the cells were visualized utilizing DAPI staining. Stained cells were observed under a confocal laser scanning microscope (Olympus FV3000, Japan) and analyzed using Image-Pro Plus image analysis software.

### Western blotting

Total proteins were extracted from cells using lysis buffer, and the protein concentration was determined using a BCA assay kit (Thermo Fisher Scientific, USA). An equal amount of protein was separated by SDS-PAGE, followed by transferring the proteins onto a polyvinylidene fluoride membrane. The membrane was blocked with 5% bovine serum albumin at room temperature for 1.5 h. Thereafter, the membrane was incubated overnight at 4°C with the corresponding primary antibodies (anti-LC3I, anti-LC3II, anti-Beclin1, anti-p62, anti-TYR, and

anti- $\beta$ -actin). Subsequently, the membrane was incubated for 1 h with horseradish peroxidase-conjugated secondary antibody diluted in TBS-T buffer containing 1% non-fat milk. Protein bands were visualized using an ECL detection kit (GE Healthcare, USA) and quantified using the Image J software. The relative expression of the target proteins was normalized against  $\beta$ -actin.

#### Transmission electron microscopy (TEM)

B16 cells were fixed in 2.5% glutaraldehyde. After fixation, cells were observed under a HT7800 transmission electron microscope (Hitachi, Japan). Autophagic vacuoles and melanosomes were analyzed under a final magnification of 2,000 $\times$  with five random fields.

#### Statistical analysis

All data are expressed as the mean  $\pm$  standard deviation (SD) derived from three independent experiments. Statistical analysis was performed utilizing GraphPad Prism version 8 software. Statistical comparisons were conducted using either a two-tailed t-test or one-way analysis of variance (ANOVA), with a threshold of  $P < 0.05$  considered statistically significant.

## Results.

### Cytotoxicity of W335 and TXA on keratinocytes and melanocytes

First, the cytotoxicity of W335 and TXA on keratinocytes (HaCaT) and melanocytes (B16) was assessed using the CCK-8 assay. Results showed that treatment with W335 in concentration below 0.01% did not affect much with regard to the HaCaT and B16 cell viability ( $\geq 80\%$ ) (**Figures 1A, B**). Meanwhile, TXA was found to be non-toxic to HaCaT cells at concentrations below 1% and to B16 cells at concentrations below 0.1% (**Figures 1C, D**).

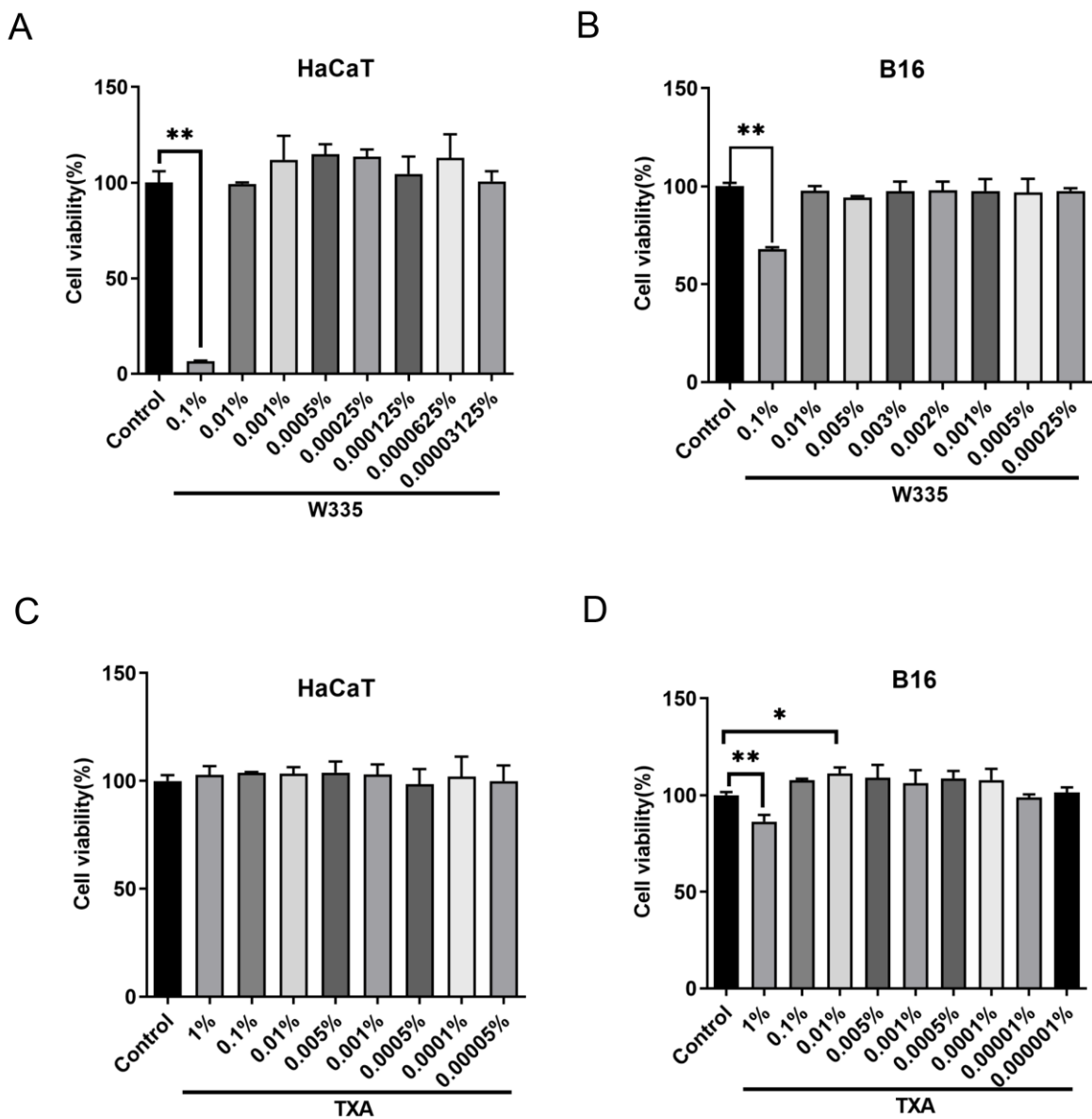


**Figure 1:** Cytotoxicity of W335 and TXA on keratinocytes and melanocytes. (A) Effect of W335 on cytotoxicity in keratinocytes (HaCaT) by CCK-8 assay. (B) Effect of W335 on cytotoxicity in melanocytes (B16). (C) Effect of TXA on cytotoxicity in HaCaT cells. (D) Effect of TXA on cytotoxicity in B16 cells. All data are expressed as the mean  $\pm$  SD ( $n=3$ ). \* indicates  $P < 0.05$  and \*\* indicates  $P < 0.01$ .

Combination of W335 and TXA suppresses melanin production in melanocytes

Based on cytotoxicity tests, three non-toxic concentrations of W335 and TXA—0.01% (high dose), 0.005% (medium dose), and 0.001% (low dose)—were selected for the analysis of melanin production. The combination of W335 and TXA at ratios of 1:2, 1:5, and 1:10 was used to treat B16 cells. **Figure 2A-C** demonstrates a significant reduction of melanin content in B16 cells treated with the medium dosage of W335 combined with TXA at a 1:10 ratio, prompting its selection for further study. Further melanin assessment manifested that both the W335 and TXA groups showed a significant reduction in melanin content compared to the control group (**Figure 3**). Notably, the combination of W335 + TXA resulted in lower melanin content in B16 cells than TXA alone (**Figure 3**). The finding indicates that the combination of W335 and TXA could further suppress melanogenesis in melanocytes than TXA alone.

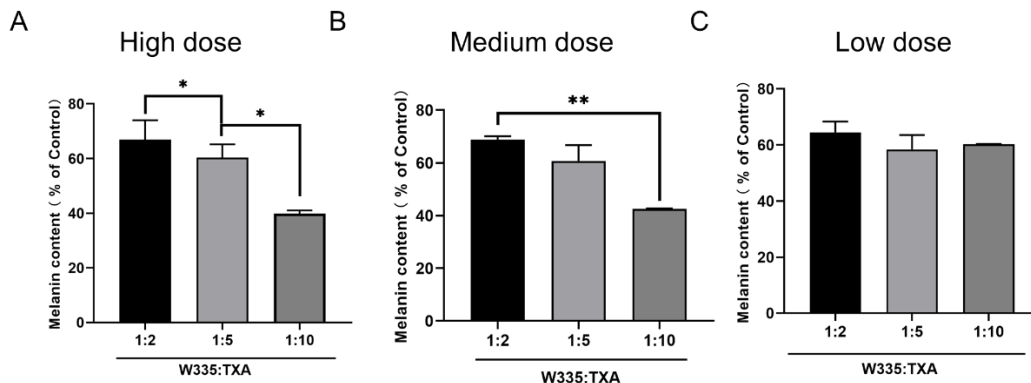


**Figure 2:** The ratios of W335 and TXA combination regulating melanin production in melanocytes.

The melanin content of B16 cells was assessed using spectrophotometry. \*indicates  $P < 0.05$  and

\*\*indicates  $P < 0.01$ .

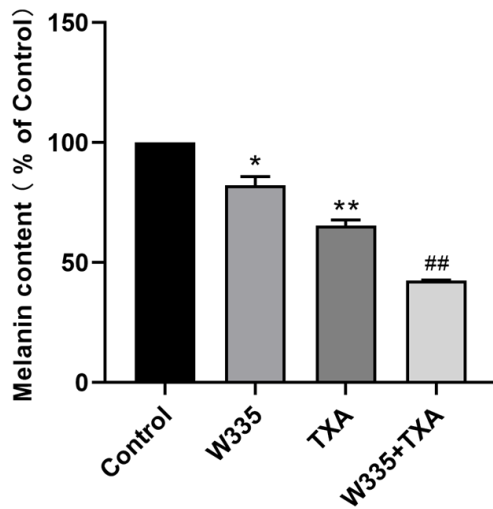


**Figure 3:** Combination of W335 and TXA suppresses melanin production in melanocytes. The melanin content of B16 cells was assessed using spectrophotometry. \* indicates  $P < 0.05$  and \*\* indicates  $P < 0.01$  when compared to the control group; ## indicates  $P < 0.01$  when compared to the TXA group.

W335 modulates the UPS and autophagy pathway

To further elucidate the molecular mechanisms of W335 inhibiting melanogenesis, RNA sequencing was conducted in melanocytes and keratinocytes treated with W335. The results showed a total of 9,197 DEGs in melanocytes after treatment with W335, comprising 4,449 upregulated and 4,748 downregulated genes (**Figure 4A**). GO enrichment analysis of DEGs revealed that UPS-related processes were significantly enriched after treatment with W335 (**Figures 4B, C**). Additionally, approximately 16% of DEGs were associated with ubiquitination (**Figure 4B, C**). In keratinocytes, there were 1,361 DEGs after treatment with W335, with 802 upregulated and 559 downregulated genes. Of note, approximately 23% of these DEGs were implicated in autophagic processes (**Figures 4E, F**). Collectively, these findings suggest that W335 might inhibit melanogenesis by regulating the UPS and autophagy pathway.

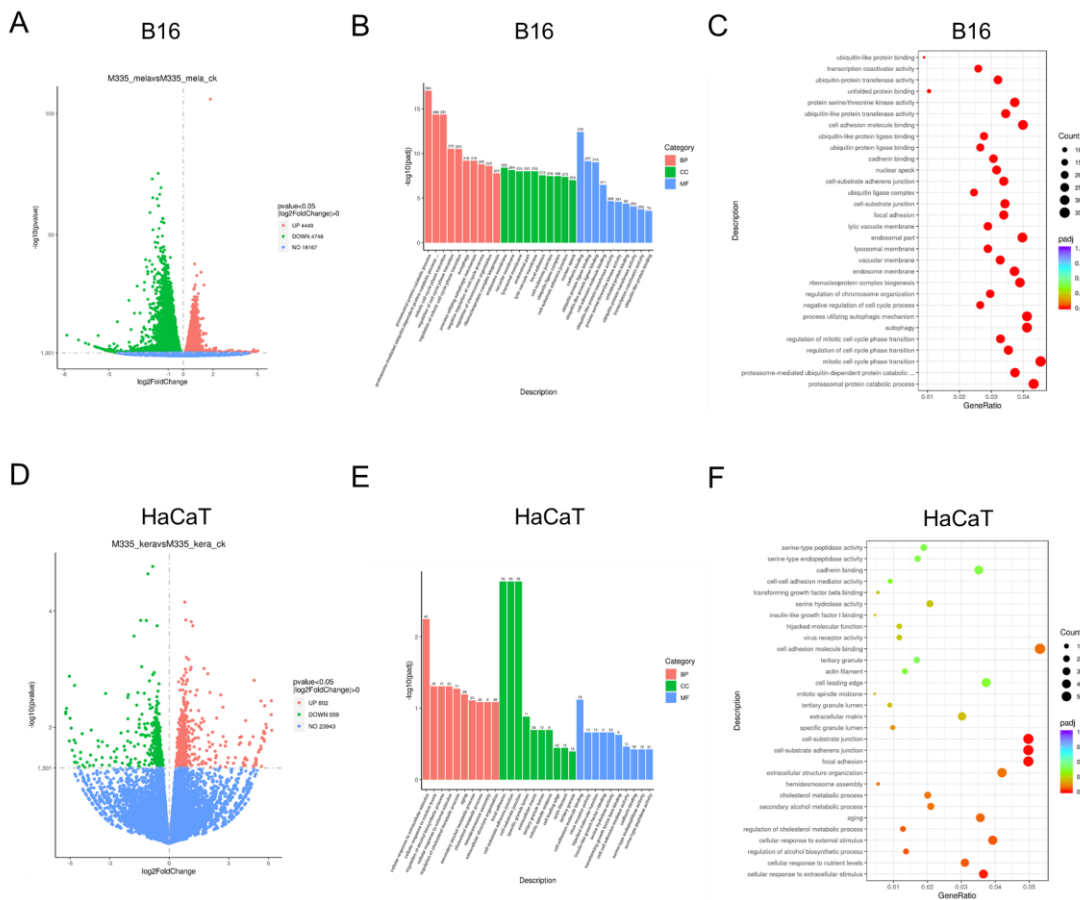


**Figure 4: Transcriptomic analysis of melanocytes and keratinocytes after treatment with W335.** (A) The volcano plot showed DEGs in melanocytes before and after W335 treatment. (B) Annotations of GO enrichment analysis for DEGs in melanocytes include biological process (BP), cellular components (CC), and molecular function (MF) categories. (C) GO enrichment scatter plot for DEGs in melanocytes. The horizontal axis represents the gene ratio, and the vertical axis represents the GO term. (D) The volcano plot showed DEGs in keratinocytes before and after W335 treatment. (E) Annotations of GO enrichment analysis for DEGs in keratinocytes include BP, CC, and MF categories. (F) GO enrichment scatter plot for DEGs in keratinocytes.

W335 and TXA combination inhibits melanogenesis by regulating the UPS  
The combination of W335 and TXA at 1:10 ratio was used for mechanism validation. As depicted in **Figure 5A**, exogenous application of the proteasome inhibitor MG132 to

melanocytes led to increased melanin content compared to W335 and/or TXA treatment. Western blot analyses revealed that treatments with W335 and/or TXA significantly reduced the TYR protein expression compared to the control group (**Figure 5B**). MG132 addition reversed the inhibitory of W335 + TXA combination on TYR expression (**Figure 5B**). Further Co-IP results showed that the content of ubiquitinated TYR was increased by W335 and/or TXA treatment or the ubiquitination activator CC-122 treatment compared to the MG132 treatment (**Figure 5C**). Moreover, immunofluorescence staining demonstrated that treatment with linoleic acid (positive control) and W335 individually induced a significant upregulation in the ubiquilin protein (UBQLN1) expression (**Figure 5D**). Notably, the combination of W335 and TXA resulted in a more significant increase in UBQLN1 protein levels compared to individual treatments (**Figure 5D**). Collectively, these findings suggest that the combination of W335 and TXA modulates the UPS to decrease TYR levels in melanocytes, thereby suppressing melanogenesis.

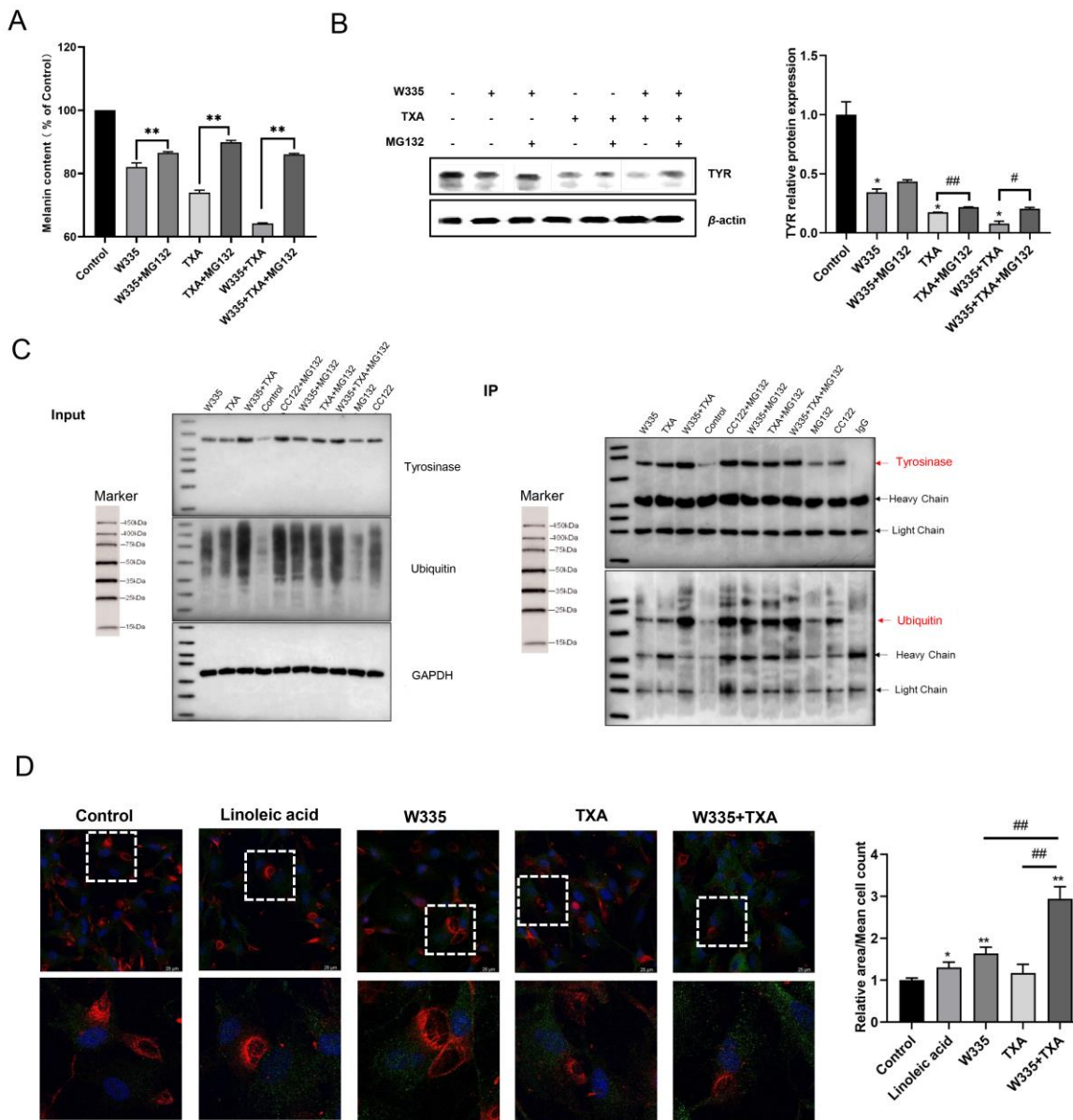


**Figure 5:** W335 and TXA combination inhibits melanogenesis by regulating the UPS. (A) The melanin content of B16 cells was assessed using spectrophotometry. \*\* indicates  $P < 0.01$ . (B) Western blot analysis of TYR protein expression in cells. \* indicates  $P < 0.05$  when compared to the control group; # indicates  $P < 0.05$  and ## indicates  $P < 0.01$ . (C) Co-IP analysis of the ubiquitination of TYR in cells. (D) Immunofluorescence staining of colocalization between ubiquilin protein UBQLN1 (green fluorescence) and TYR (red fluorescence) in cells at 63x magnification. \* indicates  $P < 0.05$  and \*\* indicates  $P < 0.01$  when compared to the control group; ## indicates  $P < 0.01$ .

W335 and TXA combination inhibits melanogenesis by activating the autophagy pathway

We further validated the involvement of autophagy pathway in the inhibition of melanogenesis by W335 and TXA combination in keratinocytes. Melanosomes were isolated from human melanoma MNT-1 cells and introduced into keratinocytes to establish a co-culture system (**Figure 6A-C**). Compared to the control group, cells treated with rapamycin (an autophagy activator), W335, or TXA exhibited a significant reduction in melanin content (**Figure 7A**). Notably, the combination of W335 and TXA treatment showed a better inhibitory effect on melanin production in keratinocytes than W335 individual treatments (**Figure 7A**). Immunofluorescence staining was performed to evaluate the expression of autophagy marker protein LC3B in keratinocytes. Compared to the control group, the expression of LC3B was increased in the rapamycin group and decreased in the hydroxychloroquine (an autophagy inhibitor) group (**Figure 7B**). Consistent with rapamycin treatment, W335 treatment led to a significant elevation in LC3B expression, alongside a marked decrease in the colocalization of LC3B and melanosomes (**Figure 7B**). Simultaneously, Western blotting showed that a significant upregulation of LC3II and Beclin-1, alongside a downregulation of p62, in cells treated with rapamycin, W335, and/or TXA. In contrast, treatment with 3-MA exerted opposing effects on these proteins (**Figure 7C**). Notably, the combination of W335 and TXA exhibited superior regulatory effects on these autophagy-related proteins than individual treatment (**Figure 7C**). Furthermore, TEM revealed that autophagosomes formed in conjunction with melanosomes. Evidently, treatments with rapamycin, W335, and/or TXA led to the degradation of melanosome structures and a reduction in melanin content within autophagosomes (**Figure 7D**). As a result, the W335 and TXA combination synergistically activates the autophagy pathway to degrade melanosomes, thereby inhibiting melanogenesis in keratinocytes.

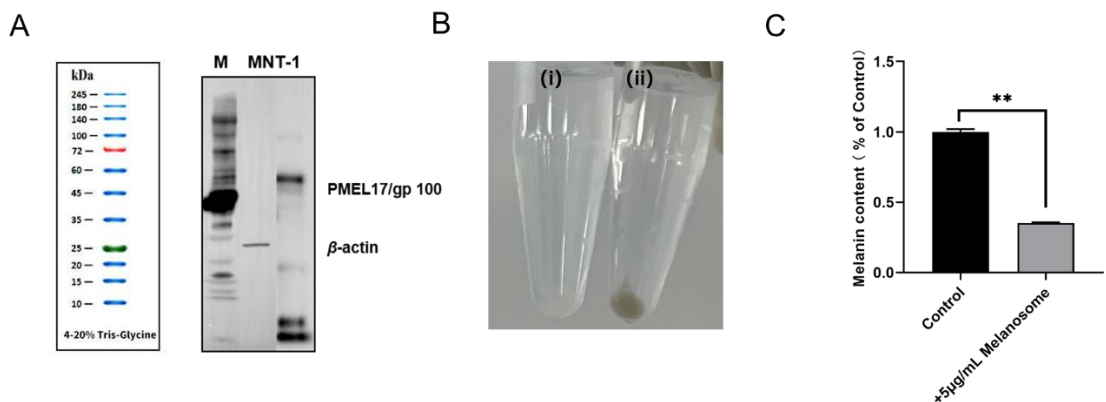


**Figure 6:** Melanosomes were isolated from human melanoma MNT-1 cells and introduced into keratinocytes to establish a co-culture system. (A) Expression of PMEL17/gp100 protein (a precursor marker for melanosomes) in MNT-1 cells. (B) Particles collected from keratinocytes only (i) and particles collected after co-cultivation with melanosomes (ii). (C) Measurement of intracellular melanin content using spectrophotometry. \*\*P < 0.01.

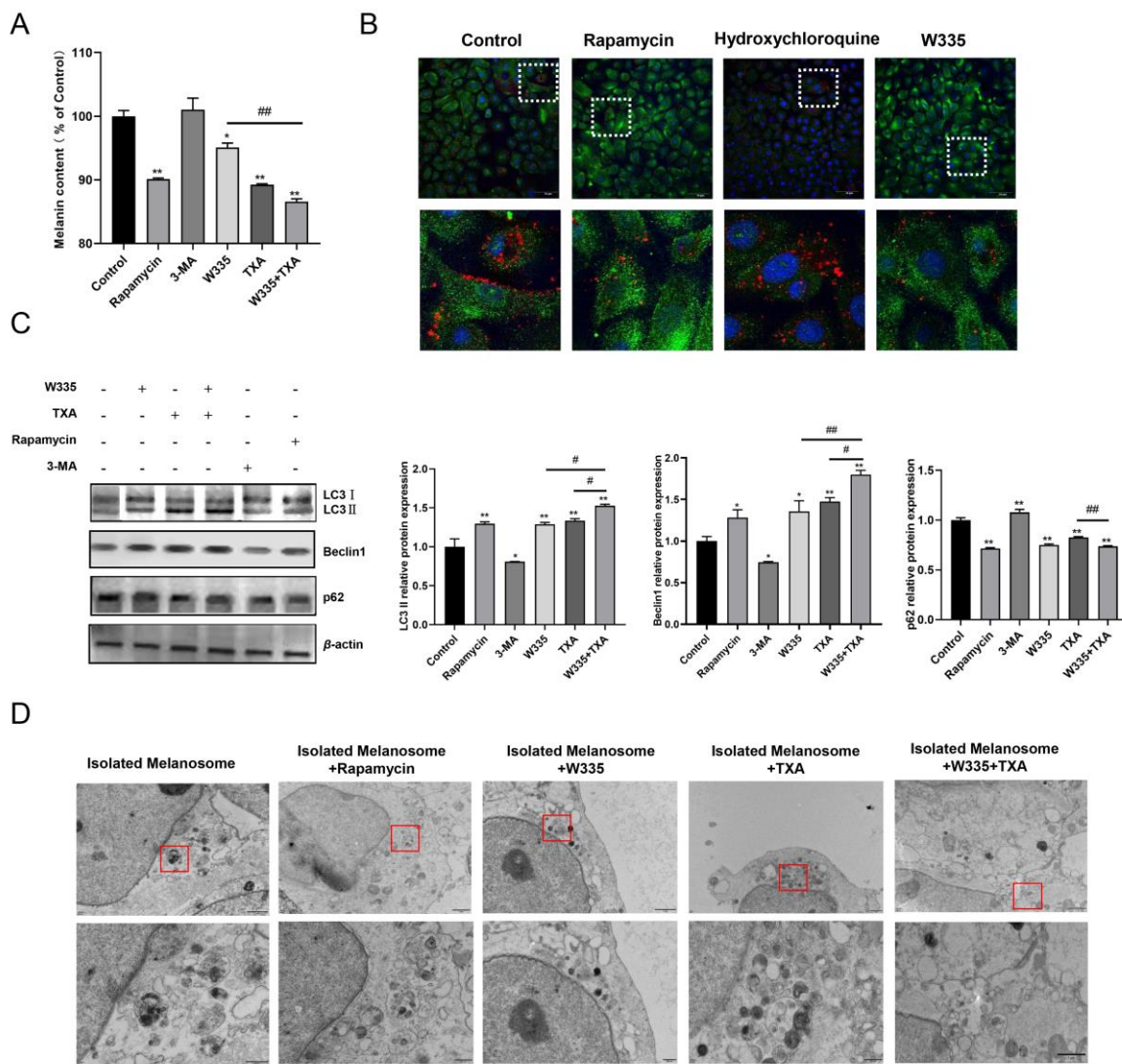


**Figure 7:** W335 and TXA combination promotes melanosome degradation by activating the autophagy pathway. Melanosomes were isolated from human melanoma MNT-1 cells and introduced into keratinocytes to establish a co-culture system. (A) The melanin content of keratinocytes was assessed using spectrophotometry. \* indicates  $P < 0.05$  and \*\* indicates  $P < 0.01$  when compared to the control group; ## indicates  $P < 0.01$ . (B) Immunofluorescence staining of colocalization between autophagy-related protein (LC3B) (green fluorescence) and melanosomes (red fluorescence) in keratinocytes at 40 $\times$  magnification. (C) Western blot analysis of the expression levels of autophagy-related proteins (LC3II/LC3I, Beclin-1, and p62). \* indicates  $P < 0.05$  and \*\* indicates  $P < 0.01$  when compared to the control group; # indicates  $P < 0.05$  and ## indicates  $P < 0.01$ .

0.01. (D) TEM was used to analyze the formation of melanosome-engulfing autophagosomes in keratinocytes.

### **Discussion.**

Pigmentation is a pivotal process in both skin physiology and the development of dermatological disorders. In previous work, we successfully synthesized the cosmetic ingredient W335 through chemical synthesis. TXA, with its established role in preventing and treating pigmentary disorders such as melasma [16], prompted us to investigate the synergistic effects and mechanisms of W335 and TXA in inhibiting melanogenesis. In this study, we uncovered that a formulation combining W335 and TXA at a ratio of 1:10 modulates the UPS to facilitate TYR degradation and activates the autophagy pathway to degrade melanosomes, thereby inhibiting melanogenesis.

The biosynthetic pathways of melanin are orchestrated through a series of enzymatic and non-enzymatic reactions. TYR, as the rate-limiting enzyme in melanogenesis, directly governs the accumulation of melanin in the skin, thereby influencing skin coloration [17]. Therefore, reducing the stability and function of TYR emerges as a promising strategy to overcome hyperpigmentation [18]. The degradation of TYR relies on both the UPS and lysosomal system. Currently, numerous skin whitening agents have been reported to regulate melanogenesis by inhibiting TYR activity; however, few have been proven to act via the UPS. Our investigation revealed that the combination of W335 and TXA facilitated ubiquitination-mediated proteasomal degradation of TYR in melanocytes, thereby inhibiting melanogenesis. Consequently, the combination of W335 and TXA has the potential to inhibit melanogenesis by regulating the stability of TYR, presenting a possible therapeutic strategy for promoting hypopigmentation. However, protein stability is also influenced by variations in degradation mechanisms, necessitating further investigation into the proteins involved in TYR ubiquitination and the respective ubiquitin binding sites.

Melanosomes are tissue-specific lysosome-related organelles of melanocytes, responsible for the synthesis and storage of melanin. Melanosome maturation progresses through four stages: I, II, III, and IV, with stages I and II representing pre-melanosomes and stages III and IV indicative of mature melanosomes [19]. Mature melanosomes accumulate at the dendrites of melanocytes and are subsequently transferred to adjacent keratinocytes. Melanin is internalized and processed within keratinocytes and then accumulated around the nuclear region to form a protective melanin cap shielding cellular DNA from UV radiation damage [20, 21]. Consequently, the processes of melanosome formation, trafficking to keratinocytes, and melanin metabolism are integral to skin pigmentation [1]. Recent studies have illuminated that autophagosome formation regulators are involved in the early stages of melanosome formation and maturation. These studies suggest that melanosomes can be degraded within melanocytes via autophagy, thereby modulating melanogenesis [22]. This study employed a co-culture model where melanosomes extracted from human MNT-1 melanoma cells were transferred to keratinocytes. The model revealed that autophagy activation decreased melanin production in keratinocytes. Importantly, treatment with W335 and TXA could effectively activate autophagy, thereby inhibiting melanogenesis.

Previous studies have demonstrated that TXA can activate the autophagy pathway by regulating autophagy-related proteins, thereby inhibiting melanogenesis [23]. Our research showed that in melanosome-containing keratinocytes, W335 and TXA treatment led to diminished LC3I conversion to LC3II, concurrently with downregulated Beclin-1 expression and upregulated p62 protein levels. LC3 and Beclin-1 are two pivotal autophagy-related proteins. The conversion of cytosolic LC3I to membrane-associated LC3II is essential for the autophagic process. Beclin-1 is indispensable for autophagosome formation, with its dysregulation resulting in abnormal autophagosome structures [24]. Similarly, p62, an autophagy adapter protein, plays a crucial role in the degradation pathway of intracellular organelles, functioning cooperatively with LC3II to facilitate selective autophagic degradation [12]. Furthermore, our

data confirmed that autophagy activation promoted melanosome degradation in keratinocytes. Notably, the combination of W335 and TXA exerts potent anti-melanogenic effects by facilitating the autophagic degradation of melanosomes. Therefore, autophagy emerges as a vital mechanism underlying the anti-melanogenic effect mediated by the combination of W335 and TXA.

### **Conclusion.**

All the results above suggested that the combination of W335 and TXA holds promise as a whitening agent in cosmetics and for the treatment of hyperpigmentation disorders, thereby presenting substantial economic potential. Our study contributes to understanding how W335 synergizes with TXA to modulate pigmentation via the UPS and autophagy, enhancing our comprehension of pigmentary disorders and informing critical strategies for skin whitening. Further investigation should concentrate on deciphering the intricate mechanisms behind TYR ubiquitination and degradation. Additionally, unraveling the details of melanosomal autophagic degradation provides fresh insights into the pathogenesis and treatment of hyperpigmentation disorders.

### **Conflict of Interest Statement.**

NONE.

### **References.**

1. Yamaguchi Y, Hearing VJ (2014) Melanocytes and their diseases. *Cold Spring Harb Perspect Med* 2014 4:a017046.
2. Ohbayashi N, Fukuda M (2020) Recent advances in understanding the molecular basis of melanogenesis in melanocytes. *F1000Res* 2020 9:F1000.
3. D'Mello SA, Finlay GJ, Baguley BC, et al (2016) Signaling Pathways in Melanogenesis. *Int J Mol Sci* 2016 17:1144.

4. Tadokoro R, Shikaya Y, Takahashi Y (2019) Wide coverage of the body surface by melanocyte-mediated skin pigmentation. *Dev Biol* 2019 449:83-89.
5. Fu C, Chen J, Lu J, et al (2020) Roles of inflammation factors in melanogenesis (Review). *Mol Med Rep* 2020 21:1421-1430.
6. Lee KW, Kim M, Lee SH, et al (2022) The Function of Autophagy as a Regulator of Melanin Homeostasis. *Cells* 2022 11:2085.
7. Zolghadri S, Beygi M, Mohammad TF, et al (2023) Targeting tyrosinase in hyperpigmentation: Current status, limitations and future promises. *Biochem Pharmacol* 2023 212:115574.
8. Su T, Yang M, Wang P, et al (2020) Interplay between the Ubiquitin Proteasome System and Ubiquitin-Mediated Autophagy in Plants. *Cells* 2020 9:2219.
9. Shi J, Guo Y, Wang H, et al (2022) The ubiquitin-proteasome system in melanin metabolism. *J Cosmet Dermatol* 2022 21:6661-6668.
10. Hu S, Wang L (2023) The potential role of ubiquitination and deubiquitination in melanogenesis. *Exp Dermatol* 2023 32:2062-2071.
11. Ji CH, Kwon YT (2017) Crosstalk and Interplay between the Ubiquitin-Proteasome System and Autophagy. *Mol Cells* 2017 40:441-449.
12. Yang Z, Klionsky DJ (2010) Mammalian autophagy: core molecular machinery and signaling regulation. *Curr Opin Cell Biol* 2010 22:124-131.
13. Murase D, Hachiya A, Takano K, et al (2013) Autophagy has a significant role in determining skin color by regulating melanosome degradation in keratinocytes. *J Invest Dermatol* 2013 133:2416-2424.
14. Ramkumar A, Murthy D, Raja DA, et al (2017) Classical autophagy proteins LC3B and ATG4B facilitate melanosome movement on cytoskeletal tracks. *Autophagy* 2017 13:1331-1347.
15. Yang HL, Lin CP, Vudhya Gowrisankar Y, et al (2021) The anti-melanogenic effects of ellagic acid through induction of autophagy in melanocytes and suppression of UVA-

- activated α-MSH pathways via Nrf2 activation in keratinocytes. *Biochem Pharmacol* 2021 185:114454.
16. Zhang L, Tan WQ, Fang QQ, et al (2018) Tranexamic Acid for Adults with Melasma: A Systematic Review and Meta-Analysis. *Biomed Res Int* 2018 2018:1683414.
17. Li L, Tang Y, Li X, et al (2023) Mechanism of skin whitening through San-Bai decoction-induced tyrosinase inhibition and discovery of natural products targeting tyrosinase. *Medicine (Baltimore)* 2023 102:e33420.
18. Brito S, Heo H, Cha B, et al (2022) A systematic exploration reveals the potential of spermidine for hypopigmentation treatment through the stabilization of melanogenesis-associated proteins. *Sci Rep* 2022 12:14478.
19. An X, Lv J, Wang F (2022) Pterostilbene inhibits melanogenesis, melanocyte dendricity and melanosome transport through cAMP/PKA/CREB pathway. *Eur J Pharmacol* 2022 932:175231.
20. Fukuda M (2021) Rab GTPases: Key players in melanosome biogenesis, transport, and transfer. *Pigment Cell Melanoma Res* 2021 34:222-235.
21. Bento-Lopes L, Cabaço LC, Charneca J, et al (2023) Melanin's Journey from Melanocytes to Keratinocytes: Uncovering the Molecular Mechanisms of Melanin Transfer and Processing. *Int J Mol Sci* 2023 24:11289.
22. Zhu W, Zhao Z, Cheng B (2020) The role of autophagy in skin pigmentation. *Eur J Dermatol* 2020 30:655-662.
23. Cho YH, Park JE, Lim DS, et al (2017) Tranexamic acid inhibits melanogenesis by activating the autophagy system in cultured melanoma cells. *J Dermatol Sci* 2017 88:96-102.
24. Kong Z, Yao T (2022) Role for autophagy-related markers Beclin-1 and LC3 in endometriosis. *BMC Womens Health* 2022 22:264.